NUMERICAL OPTIMIZATION OF COMPUTING ALGORITHMS OF THE VARIATIONAL NODAL METHOD

W. S. Yang[*], G. Palmiotti
Argonne National Laboratory
9700 South Cass Avenue
Argonne, Illinois 60439
wsyang@chosun.ac.kr; GPalmiotti@anl.gov

E. E. Lewis
Northwestern University
Department of Mechanical Engineering
Evanston, Illinois 60208
e-lewis@nwu.edu

[*]Permanent Address: Dept. of Nucl. Engineering, Chosun University,
P. O. Box 275, Kwangju, 501-600, Korea

ABSTRACT

Numerical schemes have been developed for improving the computational efficiency of the variational nodal method (VNM). Reordering and orthogonal transformation schemes for nodal unknowns have been found for reducing the coefficient matrices of VNM into block-diagonal forms. The resulting block-diagonal forms of coefficient matrices make it possible to eliminate the unnecessary operations in matrix manipulations and hence reduce the computational time. These new schemes have been incorporated within the algorithms currently used in the variational nodal code VARIANT at Argonne National Laboratory. All primary algorithms ranging from the generation of response matrices to the iterative solution scheme for the response matrix equations have been modified to implement the new schemes. The efficiency of the new schemes has been tested on eigenvalue problems by comparing the computation times of the new and existing schemes. Three-dimensional calculations were performed in hexagonal and Cartesian geometry for various spatial and angular approximations. The test results show that very significant gains can be obtained especially for the coupling coefficient calculations in higher angular approximations. Almost an order of magnitude for the total computing time is achieved in the best case.

1. INTRODUCTION

The variational nodal method,[1,2] a hybrid finite element method that guarantees nodal balance and permits spatial refinement through the use of hierarchical complete polynomial trial functions, has been successfully implemented in both the ANL neutronic code system as the VARIANT code[3] and in the European fast reactor code system ERANOS[4]. Use of VNM has allowed nearly routine performance of quite complex three-dimensional transport calculations for both fast and thermal systems. Nevertheless, VARIANT computing times tend to be more lengthy than those of the fast nodal diffusion methods most

frequently used as flux solvers in burn-up or kinetic calculations. Thus reductions in computation times would make the use of VNM more attractive for such applications. Simplified spherical harmonics provided the first successful approach to computation time reduction.[5] These simplified angular approximations yield accuracies very close to full spherical harmonics solutions with computational costs only a few times those of the corresponding diffusion solutions.

As a second approach for obtaining significant reductions in computing times, numerical schemes have been developed based on the reordering and orthogonal transformation of nodal unknowns. It has been found that the coefficient matrices of VNM can be reduced to block-diagonal forms by reordering unknowns and by applying an orthogonal transformation. The resulting block-diagonal forms of coefficient matrices make it possible to eliminate the unnecessary operations in matrix manipulations and hence reduce the computational time. These reordering and orthogonal transformation schemes have been incorporated with the algorithms currently used in the variational nodal code VARIANT at Argonne National Laboratory. All primary algorithms ranging from the generation of response matrices to the iterative solution scheme for the response matrix equations have been modified to implement the new schemes.

In what follows, we present these numerical schemes and test results. In section 2, we describe the details of the reordering and orthogonal transformation schemes for both hexagonal and Cartesian geometry. In sections 3, we present a series of three-dimensional calculations performed in hexagonal and Cartesian geometry. For various spatial and angular approximations, computational cost comparisons are made between new and existing schemes.

2. METHOLOGY

In the variational nodal methods, the final equations are cast in the following nodal response matrix equations[1]

$$\boldsymbol{j}^{+} = \mathbf{R}\boldsymbol{j}^{-} + \mathbf{B}\boldsymbol{s}, \tag{1}$$

where $\boldsymbol{j}^{+}$ and $\boldsymbol{j}^{-}$ are, respectively, outgoing and incoming partial current-like moments, each integrated over the corresponding node surface, and $\boldsymbol{s}$ contains the source moments integrated over the node volume. The response matrices $\mathbf{R}$ and $\mathbf{B}$ are defined by

$$\mathbf{R} = [\mathbf{G} + \mathbf{I}]^{-1}[\mathbf{G} - \mathbf{I}] \tag{2}$$

and

$$\mathbf{B} = [\mathbf{G} + \mathbf{I}]^{-1}\mathbf{C}, \tag{3}$$

where $\mathbf{G} = \frac{1}{2}\mathbf{M}^{T}\mathbf{A}^{-1}\mathbf{M}$ and $\mathbf{C} = \frac{1}{2}\mathbf{M}^{T}\mathbf{A}^{-1}$. Details of the matrices $\mathbf{A}$ and $\mathbf{M}$ are discussed elsewhere[3] along with the basis functions employed in the variational formulation.

To determine the response matrices for each unique node, two matrices $\mathbf{A}$ and $\mathbf{G} + \mathbf{I}$ must be inverted. For higher order transport approximations, these matrix inversions require considerable computational time, especially when a large number of node types is involved. Although the matrix $\mathbf{A}$ is a sparse symmetric matrix, its structure is not simple as shown in Figure 1.a for the P_3 approximation in

hexagonal-z geometry. However, since the angular and spatial approximations are made separately in the variational nodal method, not all the elements of $\mathbf{A}$ are connected. That is, the matrix $\mathbf{A}$ is reducible, and hence it can be transformed by a symmetric permutation (i.e., by reordering its columns and rows) into a block diagonal matrix $\tilde{\mathbf{A}}$ as

$$\tilde{\mathbf{A}} = \mathbf{P}^T \mathbf{A} \mathbf{P}, \tag{4}$$

where $\mathbf{P}$ is a permutation matrix. For example, by the reverse Cuthill-McKee reordering (RCMK)[6], the $\mathbf{A}$ matrix for the P_3 approximation in hexagonal-z geometry can be transformed into the block diagonal matrix composed of 14 sub-matrices as shown in Figure 1.b. Because of the block diagonal form, the matrix $\tilde{\mathbf{A}}$ can be inverted much more efficiently than the original matrix $\mathbf{A}$. Using the inverse of $\tilde{\mathbf{A}}$, the matrices $\mathbf{C}$ and $\mathbf{G}$ can also be computed with much less effort as $\mathbf{C} = (\mathbf{M}^T \mathbf{P}) \tilde{\mathbf{A}}^{-1} \mathbf{P}^T$ and $\mathbf{G} = \mathbf{C}\mathbf{M}$.

In contrast to the $\mathbf{A}$ matrix, the matrix $\mathbf{G}$ is not reducible as can be expected from the physical argument that all the partial currents are strongly connected. Hence, reordering of unknowns does not make the inversion of $\mathbf{G} + \mathbf{I}$ simpler. However, it can be shown that the matrix $\mathbf{G}$ is transformed into a reducible matrix by the orthogonal transformation based on the node symmetry. Since the surfaces of a node can be numbered in an arbitrary order, the change of surface numbering does not alter the values of elements of $\mathbf{G}$. It only permutes the corresponding elements of $\mathbf{G}$. In other words, the structure of $\mathbf{G}$ reflects the geometric symmetry of a node. Therefore, using the orthogonal matrix $\mathbf{X}$ composed of eigenvectors of the symmetry operators for the node geometry, the matrix $\mathbf{G}$ can be transformed to a reducible matrix $\tilde{\mathbf{G}}$ as

$$\tilde{\mathbf{G}} = \mathbf{X}^T \mathbf{G} \mathbf{X}. \tag{5}$$

The orthogonal matrix $\mathbf{X}$ is shown in Table I for the hexagonal and rectangular prism nodes. Here the surfaces of a node are numbered in the order of side surfaces (numbered counter-clockwise) and then bottom and top surfaces.

As in the case of the $\mathbf{A}$ matrix, the reducible matrix $\tilde{\mathbf{G}}$ can be transformed by the RCMK reordering into a block diagonal matrix $\hat{\mathbf{G}}$ as

$$\hat{\mathbf{G}} = \mathbf{Q}^T \tilde{\mathbf{G}} \mathbf{Q}, \tag{6}$$

where $\mathbf{Q}$ is a permutation matrix. For example, the $\mathbf{G}$ matrix shown in Figure 2.a for the P_3 approximation in hexagonal-z geometry can be transformed into the block diagonal matrix $\hat{\mathbf{G}}$ composed of 4 sub-matrices as shown in Figure 2.b. Therefore, the matrix $\hat{\mathbf{G}} + \mathbf{I}$ can be inverted much more efficiently than the original matrix $\mathbf{G} + \mathbf{I}$. Using the inverse of $\hat{\mathbf{G}} + \mathbf{I}$, the response matrices $\mathbf{R}$ and $\mathbf{B}$ can be efficiently computed as

$$\mathbf{R} = \mathbf{X}\tilde{\mathbf{R}}\mathbf{X}^T = \mathbf{X}\left[\mathbf{I} - 2\mathbf{Q}\left(\hat{\mathbf{G}} + \mathbf{I}\right)^{-1}\mathbf{Q}^T\right]\mathbf{X}^T \tag{7}$$

and

$$\mathbf{B} = \left\{ \mathbf{X} \left[\mathbf{Q} \left(\hat{\mathbf{G}} + \mathbf{I} \right)^{-1} \mathbf{Q}^{T} \right] \mathbf{X}^{T} \right\} \mathbf{C} . \tag{8}$$

The matrix $\tilde{\mathbf{R}}$ defined in Eq. (7) is much sparser than the response matrix $\mathbf{R}$. For example, only ~16% of its elements are non-zero in case of the P_3 approximation in hexagonal-z geometry. As a result, if we employ the $\tilde{\mathbf{R}}$ matrix in solving the response matrix equation given in Eq. (1) iteratively, the number of flops required in the matrix and vector multiplication ($\mathbf{R}\boldsymbol{j}^{-}$) can be reduced significantly. This can be accomplished by two orthogonal transformations of vector as

$$\mathbf{R}\boldsymbol{j}^{-} = \mathbf{X} \left[\tilde{\mathbf{R}} (\mathbf{X}^{T} \boldsymbol{j}^{-}) \right] . \tag{9}$$

Since the orthogonal matrix $\mathbf{X}$ contains only a few different elements, the multiplication of $\mathbf{X}$ and a vector requires a small number of flops. Therefore, the number of flops required for determining the right side of Eq. (9) is smaller than that for the left side. This reduction of flops increases rapidly as the matrix size increases, that is, as the order of approximation becomes higher.

3. IMPLEMENTATION AND RESULTS

Response matrix acceleration schemes based on the RCMK reordering and orthogonal transformation of nodal unknowns have been incorporated with the algorithms currently used in the variational nodal code VARIANT at Argonne National Laboratory. All primary algorithms ranging from the generation of response matrices to the iterative solution scheme for the response matrix equations have been modified to implement these schemes. The efficiency of new schemes has been tested using various eigenvalue problems. A series of three-dimensional calculations were performed in hexagonal and Cartesian geometry. For various spatial and angular approximations, computational cost comparisons are made between new and existing schemes.

In Tables II and III, the computing time in CPU seconds on a Sun SparcStation/60 workstation is compared for the three-dimensional Takeda's benchmark[7] problems 2 and 4. The computation times required for generating the response matrices and for solving the response matrix equations iteratively are separately compared. Problems 2 and 4 represent x-y-z and hexagonal-z models of a fast reactor, respectively. Detailed problem descriptions are given in reference 7. In these calculations, fourth-order complete polynomials are used for flux approximation within each node. The nodal structures are the same as those in reference 2. To examine the relative efficiency of the new schemes, calculations were performed for various angular approximations and interface conditions.

As indicated in Tables II and III, very significant gains have been obtained. Since the new schemes transform the response matrices orthogonally, the accuracy of the solution is not affected. The computing time for coupling coefficient calculations is reduced more significantly than the iteration solution time. The computational efficiency of the new scheme increases as the order of approximation becomes higher, that is, as the response matrix size increases. In the highest order approximation, the total computing time is reduced by almost an order of magnitude.

4. SUMMARY

In order to improve the computational efficiency of the variational nodal method, numerical schemes

have been developed based on the reordering and orthogonal transformation of nodal unknowns. It has been found that the coefficient matrices of VNM can be reduced to block-diagonal forms by reordering unknowns and by applying an orthogonal transformation. The resulting block-diagonal forms of coefficient matrices make it possible to eliminate the unnecessary operations in sparse matrix manipulations and hence reduce the computation time significantly. These response matrix acceleration schemes based on the RCMK reordering and orthogonal transformation of nodal unknowns have been incorporated with the algorithms currently used in the variational nodal code VARIANT at Argonne National Laboratory.

The efficiency of new schemes has been tested using various eigenvalue problems. A series of three-dimensional calculations were performed in hexagonal and Cartesian geometry. For various spatial and angular approximations, computational cost comparisons are made between new and existing schemes. The test results showed that very significant gains could be obtained especially for higher order approximations and the coupling coefficient calculations, achieving almost an order of magnitude for the total computing time in the best case.

In the future efforts will be devoted in improving the computational time of the inner iteration process. One possible approach would be by extending the implementation of red-black response matrix acceleration by transformation of interface variables[8], previously applied only to two-dimensional diffusion algorithms.

REFERENCES

[1] I. Dilber and E. E. Lewis, "Variational Nodal Methods for Neutron Transport," *Nucl. Sci. Eng*., **91**, 132 (1985).

[2] C. B. Carrico, E. E. Lewis, and G. Palmiotti, "Three-Dimensional Variational Nodal Transport Methods for Cartesian, Triangular, and Hexagonal Criticality Calculations," *Nucl. Sci. Eng*., **111**, 168 (1992).

[3] G. Palmiotti, E. E. Lewis, and C. B. Carrico, "VARIANT: VARIational Anisotropic Nodal Transport for Multidimensional Cartesian and Hexagonal Geometry Calculations," ANL-95/40, Argonne National Laboratory (1995)

[4] J. Y. Doriath et al. "Reactor Analysis Using a Variational Nodal Method Implemented in the ERANOS System," ANS Topical Meeting on Advances in Reactor Physics, Knoxville, TN (April 1994).

[5] E. E. Lewis and G. Palmiotti, "Simplified Spherical Harmonics in the Variational Nodal Method," *Nucl. Sci. Eng*. **126**, 48 (1997).

[6] J. A. George and J. W. Liu, *Computer Solution of Large Sparse Positive Definite Systems*, Prentice-Hall, Englewood Cliffs, NJ (1981).

[7] T. Takeda and H. Ikeda, "3-D Neutron Transport Benchmarks," NEACRP-1-300 OECD/NEA, Organization of Economic Cooperation and Development/Nuclear Energy Agency (March 1991)

[8] E. E. Lewis and G. Palmiotti, "Red-Black Response Matrix Acceleration by Transformation of Interface Variables," *Nucl. Sci. Eng*. **130**, 181 (1998).

Table I. Orthogonal Matrix $\mathbf{X}$ for the Hexagonal and Rectangular Prism Nodes

Hexagonal Prism Node	$\mathbf{X} = \begin{bmatrix} \frac{1}{\sqrt{6}} & \frac{1}{\sqrt{3}} & \frac{1}{\sqrt{3}} & \frac{1}{\sqrt{6}} & 0 & 0 & 0 & 0 \\ \frac{1}{\sqrt{6}} & \frac{1}{2\sqrt{3}} & \frac{-1}{2\sqrt{3}} & \frac{-1}{\sqrt{6}} & \frac{1}{2} & \frac{1}{2} & 0 & 0 \\ \frac{1}{\sqrt{6}} & \frac{-1}{2\sqrt{3}} & \frac{-1}{2\sqrt{3}} & \frac{1}{\sqrt{6}} & \frac{-1}{2} & \frac{1}{2} & 0 & 0 \\ \frac{1}{\sqrt{6}} & \frac{-1}{\sqrt{3}} & \frac{1}{\sqrt{3}} & \frac{-1}{\sqrt{6}} & 0 & 0 & 0 & 0 \\ \frac{1}{\sqrt{6}} & \frac{-1}{2\sqrt{3}} & \frac{-1}{2\sqrt{3}} & \frac{1}{\sqrt{6}} & \frac{1}{2} & \frac{-1}{2} & 0 & 0 \\ \frac{1}{\sqrt{6}} & \frac{1}{2\sqrt{3}} & \frac{-1}{2\sqrt{3}} & \frac{-1}{\sqrt{6}} & \frac{-1}{2} & \frac{-1}{2} & 0 & 0 \\ 0 & 0 & 0 & 0 & 0 & 0 & \frac{1}{\sqrt{2}} & \frac{1}{\sqrt{2}} \\ 0 & 0 & 0 & 0 & 0 & 0 & \frac{1}{\sqrt{2}} & \frac{-1}{\sqrt{2}} \end{bmatrix}$
Rectangular Prism Node	$\mathbf{X} = \begin{bmatrix} \frac{1}{\sqrt{2}} & 0 & \frac{1}{\sqrt{2}} & 0 & 0 & 0 \\ 0 & \frac{1}{\sqrt{2}} & 0 & \frac{1}{\sqrt{2}} & 0 & 0 \\ \frac{1}{\sqrt{2}} & 0 & \frac{-1}{\sqrt{2}} & 0 & 0 & 0 \\ 0 & \frac{1}{\sqrt{2}} & 0 & \frac{-1}{\sqrt{2}} & 0 & 0 \\ 0 & 0 & 0 & 0 & \frac{1}{\sqrt{2}} & \frac{1}{\sqrt{2}} \\ 0 & 0 & 0 & 0 & \frac{1}{\sqrt{2}} & \frac{-1}{\sqrt{2}} \end{bmatrix}$

[a] The surfaces of a node are numbered in the order of side surfaces (numbered counter-clockwise) and then bottom and top surfaces.

Table II. CPU Time Comparison for Takeda's Benchmark Problem 4 (Hexagonal-z Geometry)

Cases				CPU Time[a] (sec)			
Angular Approx.	Interface Approx.	Unknowns Per Node	k-eff	Components	Existing Methods	New Methods	Ratio[b]
P5	Quadratic	720	0.98253	Coupling Coefficient	2533.66	235.87	10.74
				Iteration	5060.36	656.99	7.70
				Sum	7594.02	892.86	8.51
	Linear	360	0.98483	Coupling Coefficient	629.25	75.16	8.37
				Iteration	222.18	34.38	6.46
				Sum	851.43	109.54	7.77
P3	Quadratic	288	0.98109	Coupling Coefficient	150.09	19.99	7.51
				Iteration	303.04	53.45	5.67
				Sum	453.13	73.44	6.17
	Linear	144	0.98275	Coupling Coefficient	37.23	5.17	7.20
				Iteration	28.15	7.91	3.56
				Sum	65.38	13.08	5.00
SP3[c]	Linear	48	0.98120	Coupling Coefficient	1.44	0.32	4.50
				Iteration	2.69	1.17	2.30
				Sum	4.13	1.49	2.77
	Flat	16	0.98764	Coupling Coefficient	0.55	0.13	4.23
				Iteration	0.57	0.48	1.19
				Sum	1.12	0.61	1.84
P1	Linear	24	0.96913	Coupling Coefficient	0.21	0.09	2.33
				Iteration	1.24	0.77	1.61
				Sum	1.45	0.86	1.69

[a] CPU time on Sun SparcStation 60
[b] CPU time of the existing methods / CPU time of the new methods
[c] Simplified spherical harmonics P_3 approximation

Table III. CPU Time Comparison for Takeda's Benchmark Problem 2 (Cartesian Geometry)

Cases				CPU Time[a] (sec)			
Angular Approx.	Interface Approx.	Unknowns Per Node	k-eff	Components	Existing Methods	New Methods	Ratio[b]
P5	Quadratic	540	0.97359	Coupling Coefficient	250.40	25.66	9.76
				Iteration	4995.74	633.86	7.88
				Sum	5246.14	659.52	7.95
	Linear	270	0.97364	Coupling Coefficient	99.36	10.21	9.73
				Iteration	1190.40	200.03	5.95
				Sum	1289.76	210.24	6.13
P3	Quadratic	216	0.97347	Coupling Coefficient	18.05	1.78	10.14
				Iteration	664.68	167.49	3.97
				Sum	682.73	169.27	4.03
	Linear	108	0.97349	Coupling Coefficient	6.26	0.72	8.69
				Iteration	168.69	56.94	2.96
				Sum	174.95	57.66	3.03
SP3[c]	Linear	36	0.97341	Coupling Coefficient	0.24	0.03	8.00
				Iteration	21.59	12.62	1.71
				Sum	21.83	12.65	1.73
	Flat	12	0.97429	Coupling Coefficient	0.12	0.04	3.00
				Iteration	6.83	6.33	1.08
				Sum	6.95	6.37	1.09
P1	Linear	18	0.96913	Coupling Coefficient	0.04	0.02	2.00
				Iteration	10.17	7.96	1.28
				Sum	10.21	7.98	1.28

[a] CPU time on Sun SparcStation 60
[b] CPU time of the existing methods / CPU time of the new methods
[c] Simplified spherical harmonics P_3 approximation

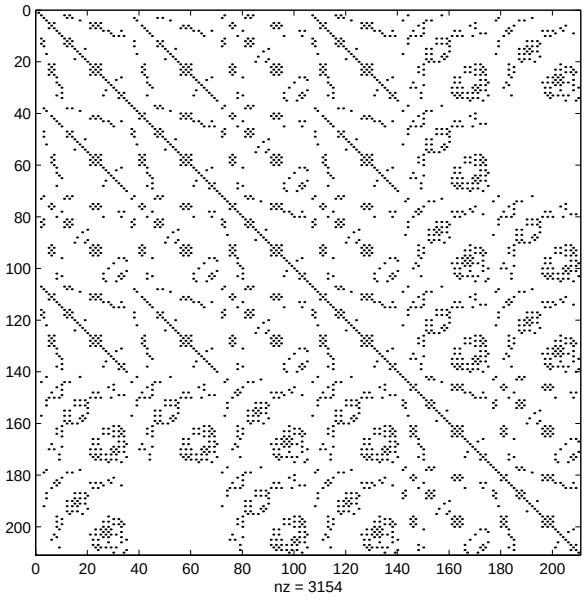

a. Original **A** Matrix

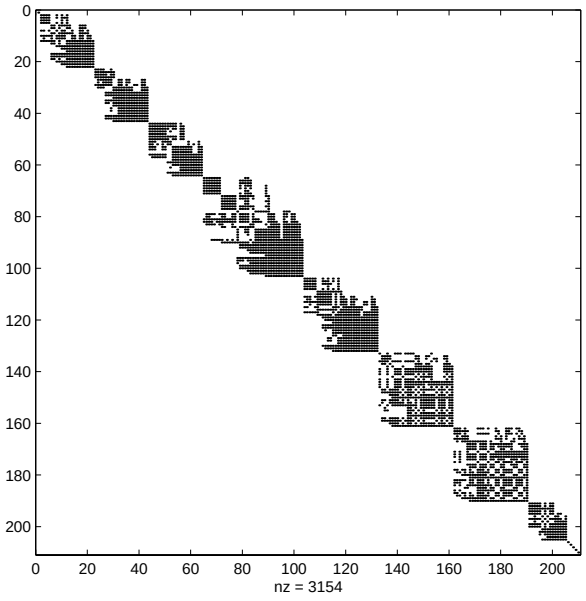

b. RCMK Ordering

Figure 1. **A** Matrix for the P_3 Approximation in Hexagonal-z Geometry

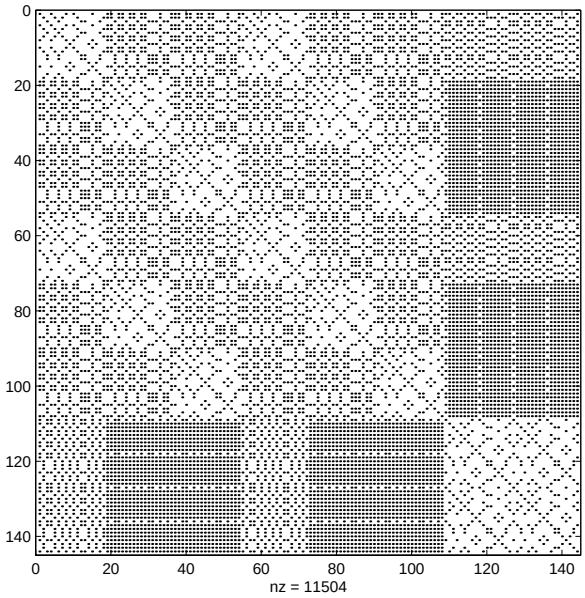

a. Original **G** Matrix

b. Orthogonal Transformation Followed by RCMK Ordering

Figure 2. **G** Matrix for the P_3 Approximation in Hexagonal-z Geometry